SPACE - TEMPORAL ANALYSIS OF LARGE GEOMAGNETIC DISTURBANCES, CASE STUDY FOR THE STORM OF 24 MARCH 2024

DINU Luminița, NICULICI Eugen Laurențiu, TĂTARU Adrian Gabriel

Abstract. Large geomagnetic disturbances are fairly rare events, even near the top of the solar cycle. These are mostly caused by particle radiation from the Sun. The flow of these particles is called solar wind. The terrestrial magnetosphere and ionosphere create magneto-hydro-dynamic waves that produce an increase in the magnetic field on the Earth's surface. The recording of the geomagnetic field is carried out in geomagnetic observatories and with the help of satellites. Magnetic observatories are permanent measuring stations that monitor geomagnetic field variations with very high precision both in time and in amplitude. Several calculation methods were used to quantify these variations, resulting in various indices of magnetic activity. They are calculated either at the planetary level or for specific areas on Earth (equatorial indices (Ae), daily indices (Ap), planetary indices (Kp), geomagnetic activity index (Dst)). In the present work, the geomagnetic storm produced on March 24, 2024 was analysed. There are situations where the different way of reporting the geomagnetic indices (Dst and Kp) can lead to the classification of the same phenomenon in two different categories (average storm after Dst and strong storm after Kp).

Keywords: solar activity, geomagnetic storm, geomagnetic indices, aurora borealis.

Rezumat. Analiza spațio – temporală a perturbațiilor geomagnetice mari, studiu de caz pentru furtuna din 24 martie 2024. Perturbațiile geomagnetice mari sunt evenimente destul de rare, chiar și în apropierea vârfului ciclului solar. Acestea sunt cauzate în mare parte de radiația particulelor provenită de la Soare. Fluxul acestor particule poartă numele de vânt solar. Magnetosfera și Ionosfera terestră creaza unde magneto-hydro-dinamice ce produc o creștere a câmpului magnetic pe suprafața Pământului. Înregistrarea câmpului geomagnetic se efectuează în observatoare geomagnetice și cu ajutorul sateliților. Observatoarele magnetice sunt stații de măsurare permanente care monitorizează variațiile câmpului geomagnetic cu precizie foarte mare atât în timp cât și în amplitudine. Pentru a cuantifica aceste variații au fost utilizate mai multe metode de calcul, rezultând diverși indici de activitate magnetică. Aceștia sunt calculați fie la nivel planetar fie pentru anumite zone de pe Pământ (indici ecuatoriali (Ae), indici zilnici (Ap), indici planetari (Kp), indicele de activitate geomagnetică (Dst)). În lucrarea de față s-a analizat furtuna geomagnetică produsă în data de 24 Martie 2024. Sunt situații în care modul diferit de raportare al indicilor geomagnetici (Dst și Kp) poate duce la încadrarea aceluiași fenomen în două categorii diferite (furtună medie după Dst și furtună puternică după Kp).

Cuvinte cheie: activitate solară, furtună geomagnetică, indici geomagnetici, aurore boreale.

INTRODUCTION

Large geomagnetic disturbances are fairly rare events, even near the peak of the solar cycle; they are mostly caused by particle radiation from the Sun. The flow of these particles is called solar wind. The interaction between the solar wind and the Earth's magnetic field creates a system of magnetospheric and ionospheric currents.

On the Earth's surface, the effects of these currents manifest as substorms, especially in the polar regions, which, in the case of strong currents, can add up to become global magnetic storms.

During solar flares, which cause magnetic storms, the energy input to the wind particles can reach 6×10^{25} Joules in a few minutes (https://ro.wikipedia.org/). For the installations on satellites located in geostationary orbits, such an event can be fatal. If the protective shielding is insufficient, some electronic components can be seriously damaged. Communication networks are also very sensitive to magnetic storms since the alteration of the stability of the ionosphere by high-energy particles alters the propagation of electromagnetic waves.

This physical phenomenon generates disturbances in the infrastructures on the ground, the corrosion process of the pipes is accelerated by the electric currents produced by the magnetic storms. However, the most serious disturbances concern the transmission of electricity. Power grids and antennas are excellent inductors for ionospheric currents. During magnetic storms, eddy currents travel through electrical cables to transformers at a high intensity that can exceed their capacity, causing transformer degradation or grid disconnection.

Depending on the intensity of the magnetic storm, the area of greatest disturbance amplitude may shift from its normal position at auroral latitudes by several degrees equatorward. During strong magnetic storms, auroras can often be observed even in mid-latitudes, radio transmissions can be disrupted and radio connections in the polar regions can be completely broken.

METHODS

The recording of the geomagnetic field is carried out in geomagnetic observatories and with the help of satellites.

Magnetic observatories are permanent measuring stations that monitor geomagnetic field variations with very high precision in both time and amplitude. These variations can have amplitudes from a few nT to hundreds or even thousands of nT at high latitudes and time durations ranging from tenths of second (pulsations) to decades (secular variation). Determining these phenomena requires the calculation of average values of components that maintain a stable rate of variation over several years and that do not contain significant anthropogenic magnetic disturbances (IANCU, 2019).

Geomagnetic observatories use a variety of magnetometers, computing processes, and other electronic devices to obtain values of the components of the Earth's magnetic field at intervals of one minute to a second. The recorded values of the components depend on the type of variometers used and the orientation of the variometer sensors. The reliability of the component values can be influenced by several factors, such as: the orientation and orthogonality of the variometer sensors, the stability of the variometer poles, the filtering method used for the digital values, the temperature coefficients (thermal stability in the variometer chamber) of the variometer sensors and other devices, the basic noise of sensors and electronics and how absolute controls are applied.

Instruments, electronics, computational processes and other observer procedures are selected so that the effects of the above factors can be minimized. Quality control procedures must be used continuously to monitor these influences.

RESULTS AND DISCUSSIONS

In the present paper we chose to analyse the geomagnetic storm produced on March 24, 2024. Fig. 1 shows 17 geomagnetic observatories located at different latitudes, and Fig. 2 shows the recordings for 4 days (March 23-26, 2024) of these observatories (***. https://intermagnet.org/). In this way, we can analyse the amplitude, the shape of each record according to the location of the observer. We can also analyse how the storm manifested itself around the globe.

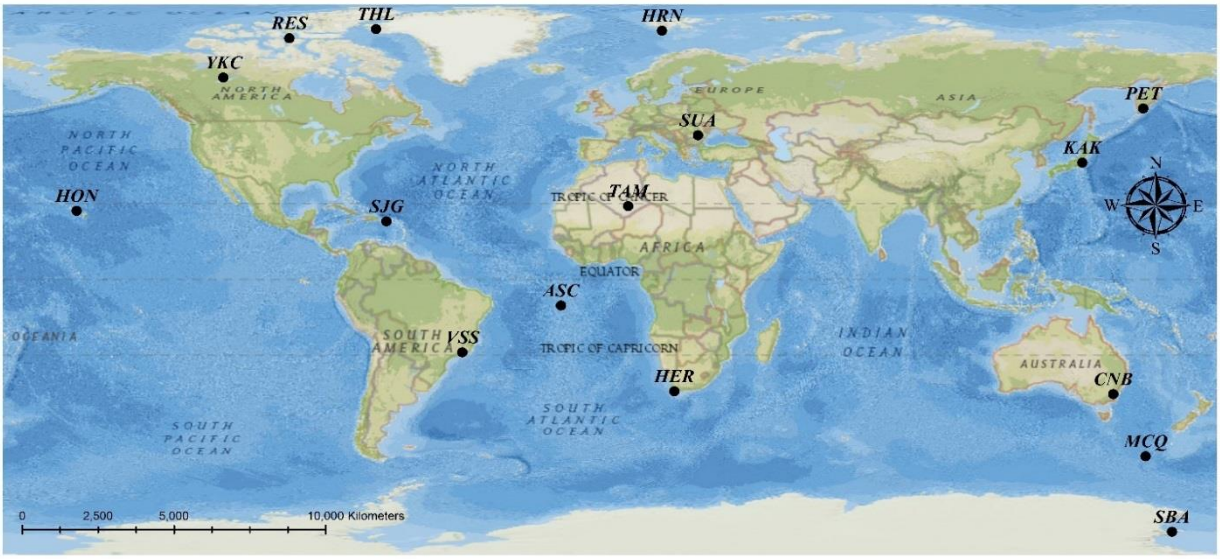

Figure 1. Positioning of the 17 geomagnetic observatories used to analyze the March 24, 2024 geomagnetic storm.

The sudden onset of storms is recorded at the same time in geomagnetic observatories, being caused by the shock wave produced on the plasma magnetosphere from the solar wind, thrown from the active areas of the Sun in the form of a stream of accelerated particles. At the same time, the intensification of solar electromagnetic radiation from the light spectrum takes place. They reach the earth in about 8 minutes, penetrate the magnetosphere, especially through the area of the magnetic poles, reaching the upper ionized layers of the atmosphere, contributing to the increase of its conductivity and therefore to the intensification of the electric current systems that produce the solar diurnal variation Sq. This effect can only be recorded at observatories located at that time in the hemisphere illuminated by the Sun and precedes the sudden onset of the storm (ssc) by several hours. The speed of the solar wind during a storm varies between 550-1200 km/sec (IANCU, 2019).

On March 23, 2024, between 14:07 and 14:22, a solar flare effect (sfe) was recorded, and on March 24, 2024, around 14:37, the sudden start of the storm occurs and we identify an ssc.

In some cases, the sudden impulse is identified with an ssc (storm sudden commencement). Ssc is a fast change of the magnetic field up or down, by a few nT or tens of nT. Ssc in general is produced by a sudden change in the pressure of the solar wind on the boundary of the front of the magnetosphere (at a distance of about 10 Earth radii). In the case of an ssc, the magnetosphere is compressed and pushed towards the Earth.

Sfe (solar flare effect) is another group of almost sudden phenomena visible in magnetic records. They occur without a certain frequency and are difficult to distinguish on magnetograms. Sfe are caused by a sudden increase in solar UV and X radiation that ionizes the upper atmosphere and intensifies electrical currents.

Sfe only appear during daylight hours. It presents ongoing asymmetry, in the sense that the maximum phase of the phenomenon is reached in a short time, followed by a slow disappearance of it that takes place over a longer time interval. The phenomenon takes minutes or tens of minutes.

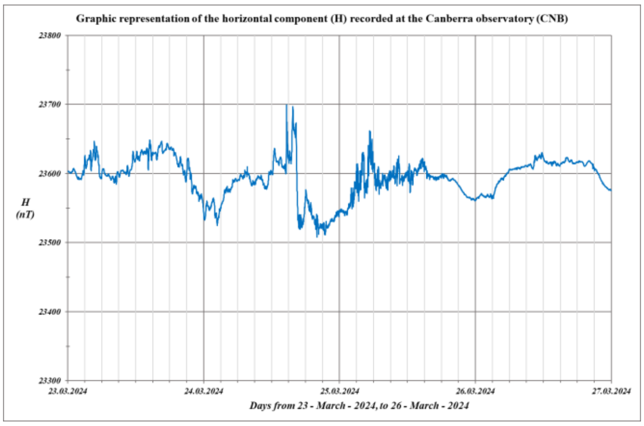
Graphic representation of the horizontal component (H) recorded at the Canberra observatory (CNB)
23800
23700
23600
23500
23400
23300
H
(nT)
23.03.2024
24.03.2024
25.03.2024
26.03.2024
27.03.2024
Days from 23 - March - 2024, to 26 - March - 2024

a)

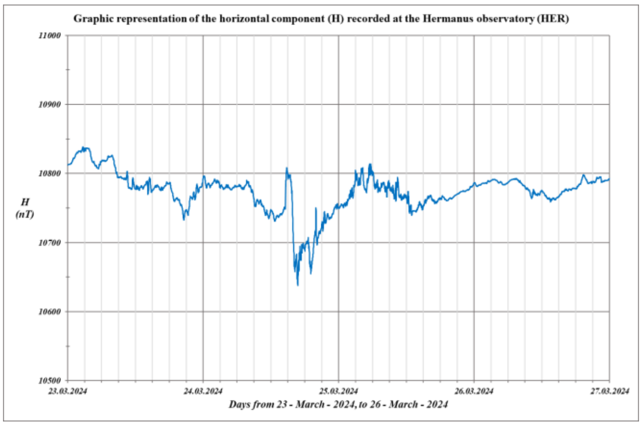
Graphic representation of the horizontal component (H) recorded at the Hermanus observatory (HER)
11000
10900
10800
10700
10600
10500
H
(nT)
23.03.2024
24.03.2024
25.03.2024
26.03.2024
27.03.2024
Days from 23 - March - 2024, to 26 - March - 2024

b)

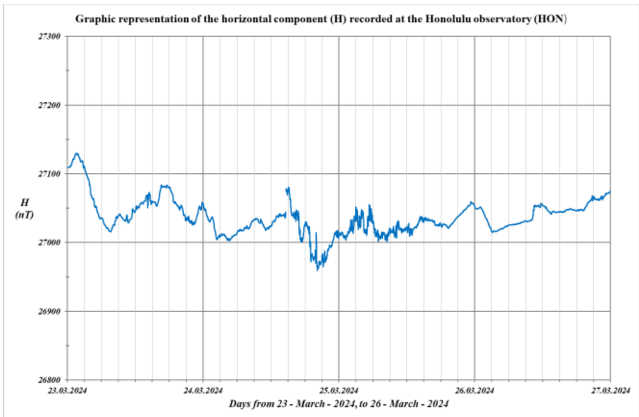
Graphic representation of the horizontal component (H) recorded at the Honolulu observatory (HON)
27300
27200
27100
27000
26900
26800
H
(nT)
23.03.2024
24.03.2024
25.03.2024
26.03.2024
27.03.2024
Days from 23 - March - 2024, to 26 - March - 2024

c)

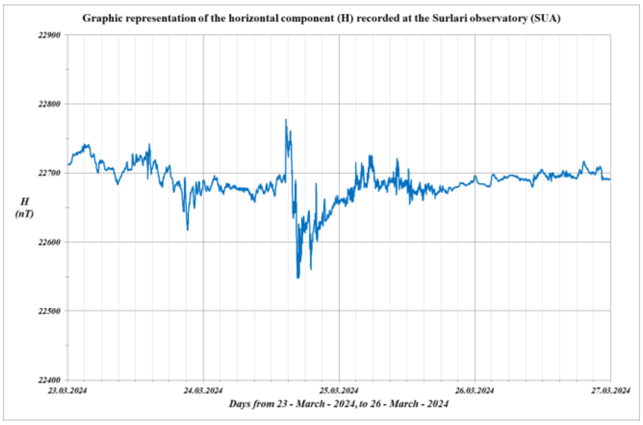
Graphic representation of the horizontal component (H) recorded at the Surlari observatory (SUA)
22900
22800
22700
22600
22500
22400
H
(nT)
23.03.2024
24.03.2024
25.03.2024
26.03.2024
27.03.2024
Days from 23 - March - 2024, to 26 - March - 2024

d)

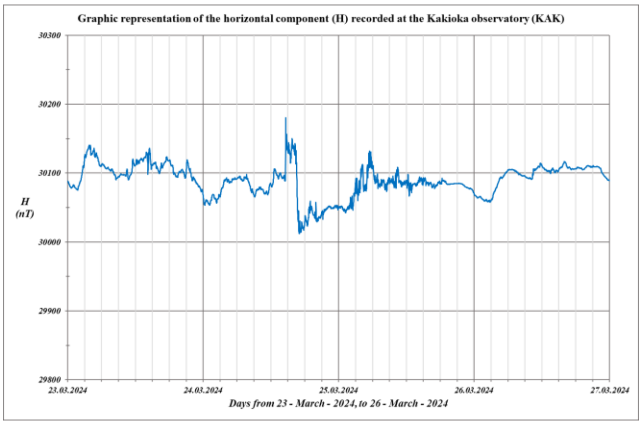
Graphic representation of the horizontal component (H) recorded at the Kakioka observatory (KAK)
30300
30200
30100
30000
29900
29800
H
(nT)
23.03.2024
24.03.2024
25.03.2024
26.03.2024
27.03.2024
Days from 23 - March - 2024, to 26 - March - 2024

e)

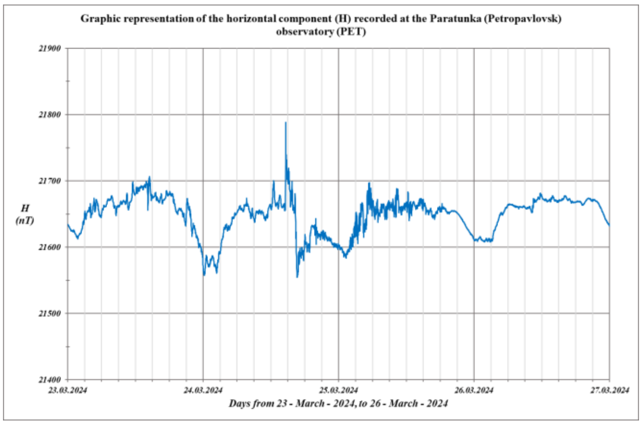
Graphic representation of the horizontal component (H) recorded at the Paratunka (Petropavlovsk) observatory (PET)
21900
21800
21700
21600
21500
21400
H
(nT)
23.03.2024
24.03.2024
25.03.2024
26.03.2024
27.03.2024
Days from 23 - March - 2024, to 26 - March - 2024

f)

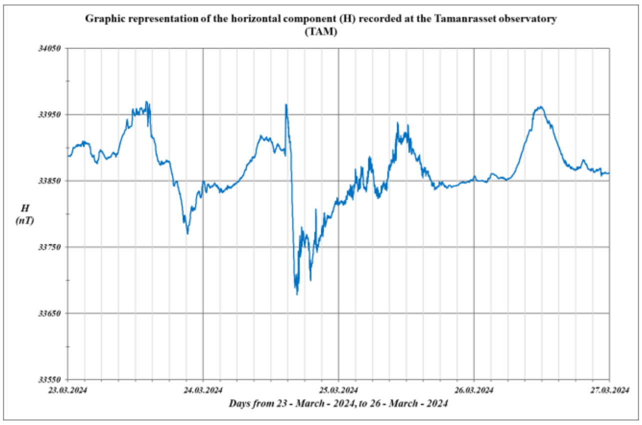
Graphic representation of the horizontal component (H) recorded at the Tamanrasset observatory (TAM)
34050
33950
33850
33750
33650
33550
H
(nT)
23.03.2024
24.03.2024
25.03.2024
26.03.2024
27.03.2024
Days from 23 - March - 2024, to 26 - March - 2024

g)

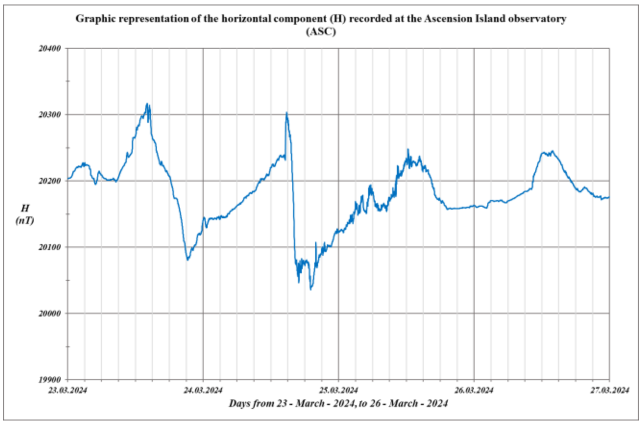
Graphic representation of the horizontal component (H) recorded at the Ascension Island observatory (ASC)
20400
20300
20200
20100
20000
19900
H
(nT)
23.03.2024
24.03.2024
25.03.2024
26.03.2024
27.03.2024
Days from 23 - March - 2024, to 26 - March - 2024

h)

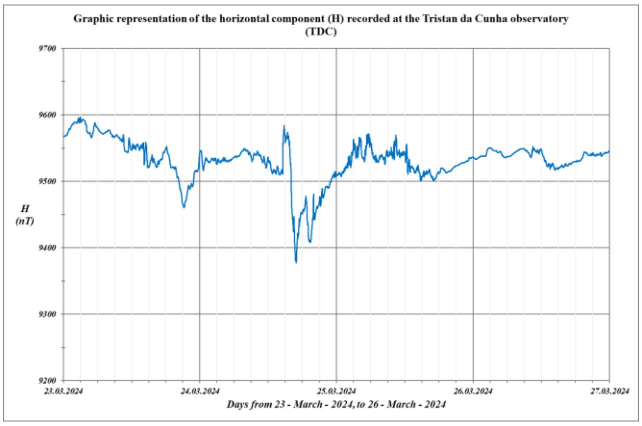
Graphic representation of the horizontal component (H) recorded at the Tristan da Cunha observatory (TDC)
9700
9600
9500
9400
9300
9200
H (nT)
23.03.2024
24.03.2024
25.03.2024
26.03.2024
27.03.2024
Days from 23 - March - 2024, to 26 - March - 2024

i)

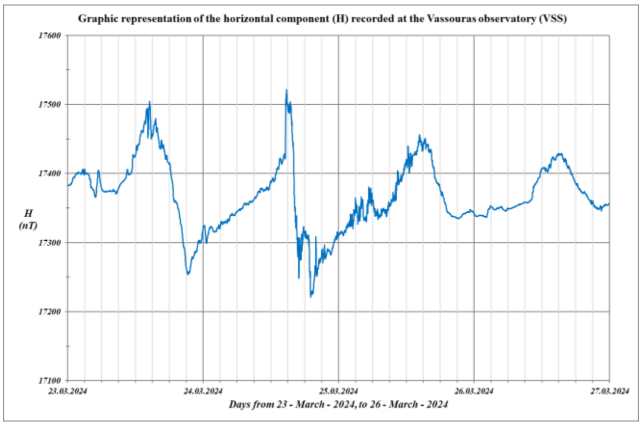
Graphic representation of the horizontal component (H) recorded at the Vassouras observatory (VSS)
17600
17500
17400
17300
17200
17100
H (nT)
23.03.2024
24.03.2024
25.03.2024
26.03.2024
27.03.2024
Days from 23 - March - 2024, to 26 - March - 2024

j)

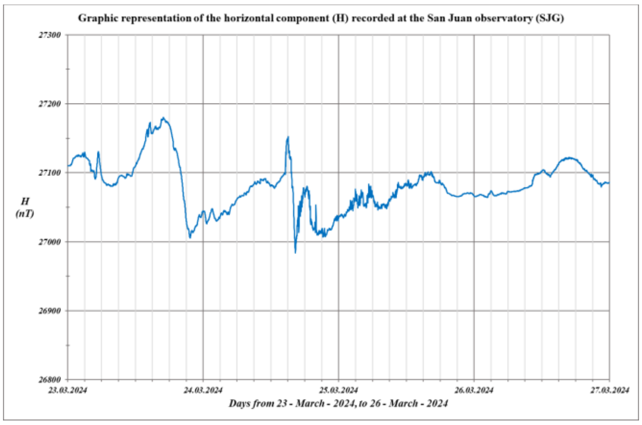
Graphic representation of the horizontal component (H) recorded at the San Juan observatory (SJG)
27300
27200
27100
27000
26900
26800
H (nT)
23.03.2024
24.03.2024
25.03.2024
26.03.2024
27.03.2024
Days from 23 - March - 2024, to 26 - March - 2024

k)

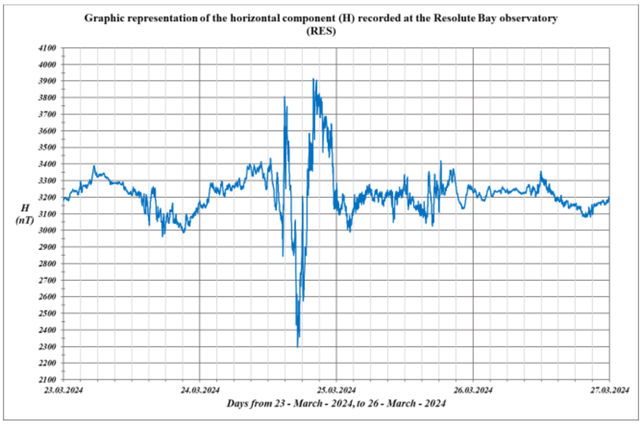
Graphic representation of the horizontal component (H) recorded at the Resolute Bay observatory (RES)
H (nT)
23.03.2024
24.03.2024
25.03.2024
26.03.2024
27.03.2024
Days from 23 - March - 2024, to 26 - March - 2024

l)

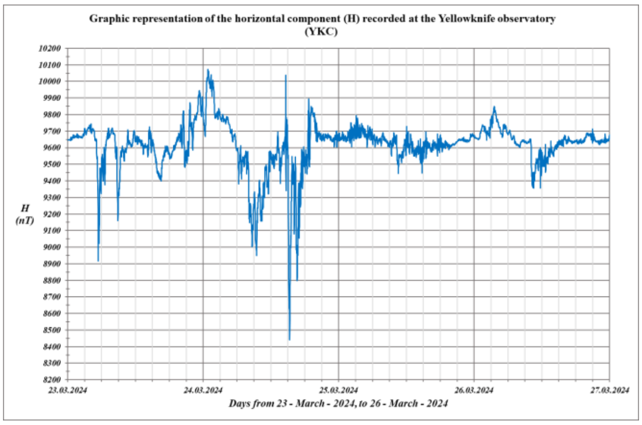
Graphic representation of the horizontal component (H) recorded at the Yellowknife observatory (YKC)
H (nT)
23.03.2024
24.03.2024
25.03.2024
26.03.2024
27.03.2024
Days from 23 - March - 2024, to 26 - March - 2024

m)

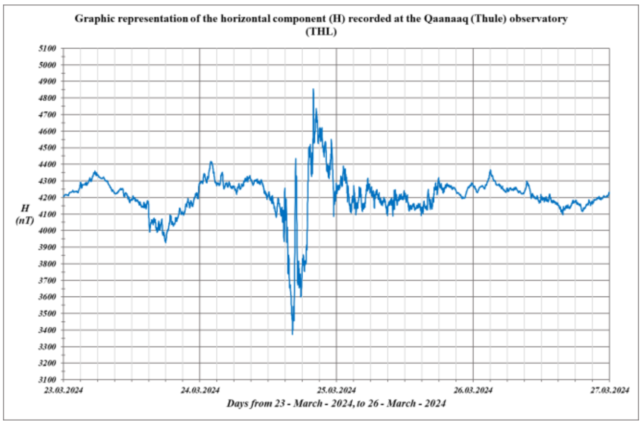
Graphic representation of the horizontal component (H) recorded at the Qaanaaq (Thule) observatory (THL)
H (nT)
23.03.2024
24.03.2024
25.03.2024
26.03.2024
27.03.2024
Days from 23 - March - 2024, to 26 - March - 2024

n)

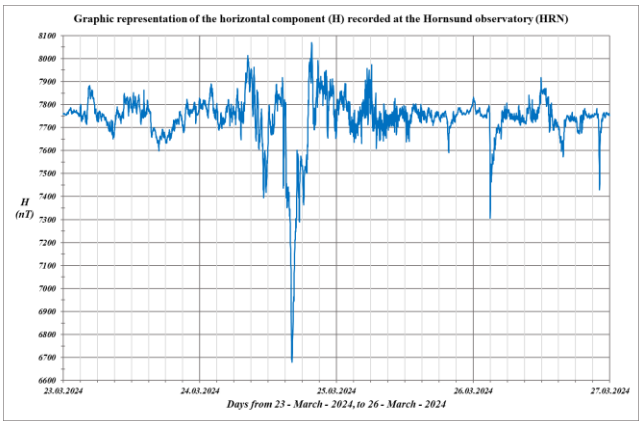
Graphic representation of the horizontal component (H) recorded at the Hornsund observatory (HRN)
H (nT)
23.03.2024
24.03.2024
25.03.2024
26.03.2024
27.03.2024
Days from 23 - March - 2024, to 26 - March - 2024

o)

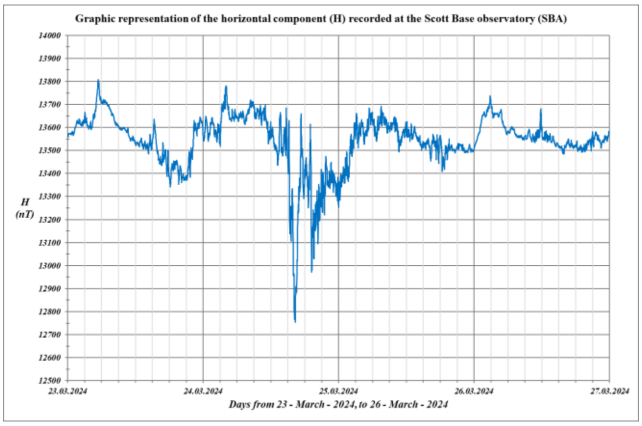
Graphic representation of the horizontal component (H) recorded at the Scott Base observatory (SBA)
H (nT)
23.03.2024
24.03.2024
25.03.2024
26.03.2024
27.03.2024
Days from 23 - March - 2024, to 26 - March - 2024

p)

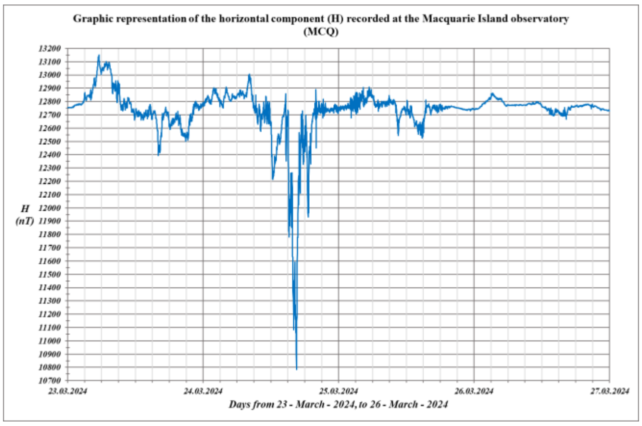

q)

Figure 2. Graphic representation of the horizontal component (H) for the period 23-26 March 2024, recorded at the geomagnetic observatory (original):
a) Camberra; b) Hermanus; c) Honolulu; d) Surlari; e) Kakioka; f) Paratunka; g) Tamanrasset; h) Ascension Island; i) Tristan da Cunha; j) Vassouras; k) San Juan; l) Resolute Bay; m) Yellowknife; n) Qaanaaq (Thile); o) Hornsund; p) Scott Base; q) Macquarie Island.

To characterize a geomagnetic storm, geomagnetic indices are used: the K/Kp index, the Ap index, the AE index and the Dst index (MAYAUD, 1980; RANGARAJAN, 1989; CAMPBELL, 2003).

The Dst index, (***. https://wdc.kugi.kyoto-u.ac.jp/dstdir/) introduced by Sugiura in 1964, represents the axially symmetric perturbation of the magnetic field at the Earth's surface at the dipole equator. Major perturbations of the Dst index are negative, indicating decreases in the geomagnetic field. Currently Dst is obtained from records of the horizontal component of the magnetic field from four low-latitude magnetic observatories. The four observatories are: Honolulu (HON), San Juan (SJG), Hermanus (HER) and Kakioka (KAK) (DINU et al., 2023).

The K indices, proposed by 13 geomagnetic observatories, distributed in different areas of the globe, are used to calculate the planetary indices Kp, currently used in the study of planetary scale phenomena. The calculation of the planetary indices Kp and their linear equivalent, the Ap indices, is carried out every month by ISGI (***. https://isgi.unistra.fr/). The Kp indices have a denser evaluation scale than the K indices and therefore intermediate values are introduced, marked with + or – (GFZ -Potsdam, 2006), (***. https://www.gfz-potsdam.de/).

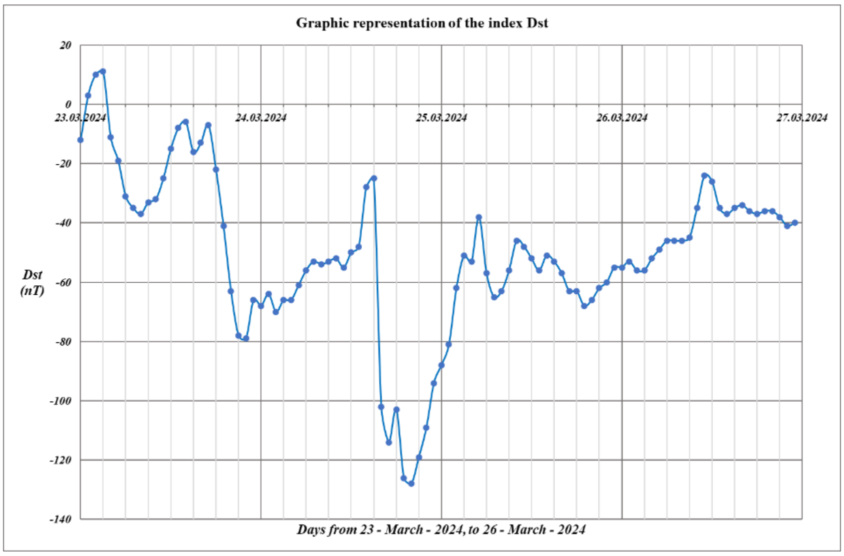

Figure 3. Graphic representasion of the index Dst for the period 23 – 26 March 2024 (original).

If we consider the storm index Dst we can classify storms into three categories (storms of low intensity, where Dst: -50 ÷ - 100, medium storms Dst: - 100 ÷ - 150 and strong storms where Dst ≤ - 150). This storm can be considered a storm of medium intensity because the Dst index had a minimum value of -128 nT (Fig. 3).

The number of sunspots on March 24, 2024 was 161, while the planetary index Kp had the value of 8,333 (Fig. 4) out of a total of 9, which indicates a strong storm.

Although the Dst index classifies the storm as of medium intensity, the large volume of particles ejected by the Sun during the explosions that produced the storm and the large extent of the areas where aurora-type phenomena were observed provide indications for its classification among geomagnetic phenomena of importance special.

Depending on the positioning of the geomagnetic observatory on the surface of the globe, the maximum amplitude of storms can range from several hundred nT at mid-latitudes to 1500 nT at flat observatories near the magnetic poles.

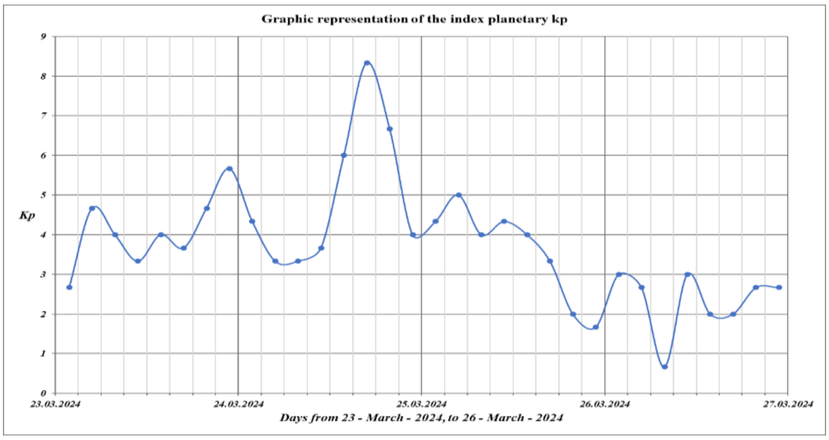

Figure 4. Graphic representation of the index planetary Kp for the period 23 – 26 March 2024.

CONCLUSIONS

At this moment, we are in the maximum phase of Solar activity cycle number 25. In the last two solar cycles, the activity of the Sun was much less than that of the current cycle.

Storms are magnetic phenomena of a planetary extent, they can affect ground-level infrastructures differently depending on their position on the globe, respectively the amplitude of the storm and the induced magnetic currents.

Although auroras are common at high latitudes, when associated with extreme geomagnetic storms, they can be seen at much lower latitudes.

The presence of auroras at mid-latitudes (45°, in the case of Romania) may suggest the possibility of affecting communication systems at lower latitudes than in the case of geomagnetic storms so far.

There are situations where the different way of reporting the geomagnetic indices (Dst and Kp) can lead to the classification of the same phenomenon in two different categories (average storm according to Dst and strong storm according to Kp). From the point of view of the Dst index, the strongest storm in the last 7 solar cycles occurred in March 1989 and had an amplitude of approximately -590 nT.

ACKNOWLEDGEMENTS

This work was supported by the Installation and Special Objective of National Interest (IOSIN) - Surlari National Geomagnetic Observatory, as well as by the National Program PN 23 39 04 01, 04/2024.

REFERENCES

CAMPBELL W. H. 2003. *Introduction to Geomagnetic Fields. Second Edition.* Cambridge University Press. 337 pp.

DINU L., NICULICI E. L., FILIPCIUC C. 2023. The use of Ap geomagnetic indices for the characterization and ranking of major geomagnetic disturbances from 1932 to 2022. *Oltenia. Studii şi comunicări. Ştiinţele Naturii*. Muzeul Olteniei Craiova. **39**(2): 44-50.

IANCU L. 2019. *Studiul variaţiei temporale a fenomenelor geomagnetice tranzitorii de perioadă scurtă din date de observator.* Teză de doctorat. Facultatea de Geologie şi Geofizică. Universitatea din Bucureşti. 292 pp.

MAYAUD P. N. 1980. *Derivation, meaning, and use of geomagnetic indices*. Geophysical Monograph Series. American Geophysical Union. Washington D. C. **22**. 154 pp,

RANGARAJAN G. K. 1989. Indices of geomagnetic activity. Cap. 5. in Jacobs J. A. (ed.): *Geomagnetism*. Academic Press. London. **3**: 385-460.

SUGIURA M. 1964. Hourly values of equatorial Dst for the IGY. *Annals of the international geophysical year*. Pergamon Press. Oxford. **35**. 269 pp.

***. https://isgi.unistra.fr/ (accessed January, 2024).

***. https://ro.wikipedia.org/ (accessed January, 2024).

***. https://www.gfz-potsdam.de/ (accessed January, 2024).

***. https://wdc.kugi.kyoto-u.ac.jp/dstdir/ (accessed January, 2024).

***. https://intermagnet.org/ (accessed January, 2024).

Dinu Luminița, Niculici Eugen Laurențiu, Tătaru Adrian Gabriel
Geological Institute of Romania, 1st Caransebeş Street, 012271 - Bucharest, Romania.
E-mails: luminita_iancu84@yahoo.com; niculicie@yahoo.com; adriantataru@live.com

Received: April 15, 2024
Accepted: August 14, 2024